

HIGH BRIGHTNESS ELECTRON SOURCES

J.B. Rosenzweig

UCLA Dept. of Physics and Astronomy, Los Angeles, CA 90095

Abstract

The production of unprecedentedly high brightness electron beams is a critical aspect of many applications, from free-electron lasers to advanced accelerators. The preferred method for obtaining these beams is the radio-frequency photoinjector. The physics and technology aspects of this device are reviewed here, along prospects for future progress in high-brightness beam development.

1 APPLICATIONS

Several applications of high brightness electron beams are driving the worldwide development of electron sources. These include free-electron sources of coherent radiation, such as self-amplified spontaneous emission free-electron lasers [1] (SASE FEL) and Compton scattering sources [2]. In the FEL, the beam is the lasing medium, and must thus be very dense to provide high gain. A measure of this is the brightness, which is the ratio of the current (linear density) to the square normalized rms emittance

$$B \equiv \frac{2I}{\epsilon_n^2}. \quad (1)$$

The brightness is a measure of the practical focusability of a beam. Other applications include very high peak current, short pulse, and moderately low emittance beams which are needed to drive wake-field accelerators [3], and linear collider sources of polarized electrons [4]. For the FEL and wake-field accelerator, a high-brightness, picosecond electron beam is a critical technology. The need for these sources in linear colliders is not as clear, as positron sources are additionally needed, and the necessary emittances may not be achieved without damping rings.

The demanded parameters for typical future applications are given in Table 1. The pulse lengths needed are given in the absence of pulse compression, which may be necessary for all applications. The parameters for the TESLA linear collider may be approachable by electron sources using slightly exotic, asymmetric rf structures [5]; for other designs, damping rings will be required.

Table 1: Electron source parameters for applications. Emittance and pulse duration are rms quantities.

Application	I (A)	ϵ_n (mm-mrad)	σ_t (psec)
SASE FEL	200	<2	<3
Wake driver	>1000	<100	<2
TESLA-LC (polarized)	800	1 (y), 20 (x)	<3

2 RF PHOTOINJECTORS

The state-of-the-art in high brightness electron sources is achieved with the rf photoinjector. This type of device, an example of which is shown in Figure 1 (the Neptune photoinjector at UCLA [6]), uses a photocathode source embedded in a high gradient rf gun. The laser pulse which excites photoemission in the gun is very short, at the level of picoseconds or below. For promptly emitting photocathodes this implies that one can create the psec electron pulses of the sort given in Table 1 in this device.

The gun is followed by a transverse focusing element (usually a solenoid), which aids in beam size and emittance control. It additionally must be post-accelerated to bring the beam to a usable energy, and to mitigate space-charge effects. This acceleration is accomplished in a booster linac, which may be physically separated, or integrated into the same rf structure as the gun.

As the effects of space-charge and wake-fields during the acceleration process often conspire to lengthen the pulse. Because of this, it is often necessary to include in the rf photoinjector system a magnetic chicane [7] for pulse compression. The chicane can give additional capabilities and design flexibility in advanced electron sources.

The analysis, design, and operation of rf photoinjector sources entail a working understanding of many diverse areas of beam physics, and accelerator and laser technology. We begin by discussing the physics of these beams, which is dominated by space-charge and violent acceleration effects.

3 PHOTOINJECTOR BEAM PHYSICS

3.1 Longitudinal dynamics

The longitudinal dynamics in an rf photoinjector are characterized by violent acceleration. This is due to two effects: the need to mitigate detrimental space-charge effects, and the requirement that the beam be captured in the rf wave within the initial cell of the standing wave rf cavity. This can be quantified by defining a unitless parameter which must exceed approximately unity [8]

$$\alpha \equiv \frac{eE_0}{2k_{RF}m_e c^2} = \frac{\gamma'}{k_{RF}} > 1 \quad (2)$$

This parameter allows a classification of injector types: high gradient injectors have $\alpha \approx 1.5 - 2.5$, whereas the lowest gradient injectors operate with $\alpha \approx 1$. The typical range of peak on-axis accelerating field encountered for a common rf wavelength, $\lambda_{RF} \equiv 2\pi/k_{RF} = 10.5$ cm, is $eE_0 = 60 - 150$ MeV/m. These high gradients allow good

control of the beam dynamics, but only within limits, as the space-charge field at the cathode due to the surface charge density there can easily be near the applied rf field. Thus we have the requirement

$$E_0 \gg 4\pi e \Sigma_b = 2eN_b / \sigma_r^2 . \quad (3)$$

This inequality guarantees only that the beam fields are perturbative. If in addition we wish to ensure that the beam not lengthen appreciably during acceleration, then we require a short acceleration length $\gamma'^{-1} = (k_{RF} \alpha)^{-1}$,

$$c\sigma_t \geq \gamma'^{-1} . \quad (4)$$

When inequalities 3 and 4 are satisfied, the beam pulse length may be preserved, and even compressed by rf focusing effects during capture in the initial cell.

Longitudinal bunch compression in photoinjectors is now a commonly employed, yet not completely understood, tool. Magnetic chicanes have been employed in a number of photoinjector facilities; space-charge limits on compressibility, and the effects of non-inertial space-charge and radiation fields on emittance growth [9] are the subjects of present and future experiments.

3.2 Transverse dynamics

Violent acceleration carries with it large transverse forces, which for an accelerator cavity terminate on a conducting (cathode) plane, gives a net first order kick to an off-axis accelerating particle. Further, this kick is rf phase dependent, and thus for a finite pulse length beam, an effective “rf” emittance is [8]

$$\varepsilon_{RF} \propto \gamma k_{RF}^2 \sigma_r^2 \sigma_z^2 \propto \alpha k_{RF}^3 \sigma_r^2 \sigma_z^2 . \quad (5)$$

The first order rf kick can be thought of as originating at the end of the structure. All other irises in the rf structure have a balance in first order inward/outward kicks, but have a second order alternating gradient focusing (of strength $\propto \gamma'^2$) [10]. The combined effect of the rf focusing can be included in envelope and matrix treatments of the beam dynamics. The analytical model has been recently verified experimentally [11].

Photoinjector beams are generally space-charge dominated. The rms envelope equation, including acceleration and space charge, can be written as

$$\sigma'' + \left(\frac{\gamma'}{\gamma} \right) \sigma' + \left[k_\beta^2 + \frac{\eta}{8} \left(\frac{\gamma'}{\gamma} \right)^2 \right] \sigma = \frac{I}{2I_0 \gamma^3 \sigma} + \frac{\varepsilon_n^2}{\gamma^2 \sigma^3} . \quad (6)$$

The emittance term is negligible for these beams (cold plasma, or quasi-laminar flow limit), with ratio of defocusing terms

$$\rho = \frac{I \sigma^2}{2I_0 \gamma \varepsilon_n^2} \gg 1 . \quad (7)$$

For high-brightness beams this situation persists until the beam is very energetic (>100 MeV), or at tight focus.

As the enclosed current in bunched beams depends on longitudinal position, or “slice”, within the bunch, the differential defocusing of the slices can produce a sheared total projected phase space. This leads to emittance growth, or, in systems with proper external focusing, emittance oscillations.

A useful heuristic model for understanding the process of emittance oscillations is shown in Figure 2. In this case, we suppose that a beam is injected with size smaller than the equilibrium sizes of the slices. As the equilibria in amplitude are dependent on the current at a given slice, the subsequent oscillations are larger for smaller currents, but the (plasma) frequency of oscillation is the same

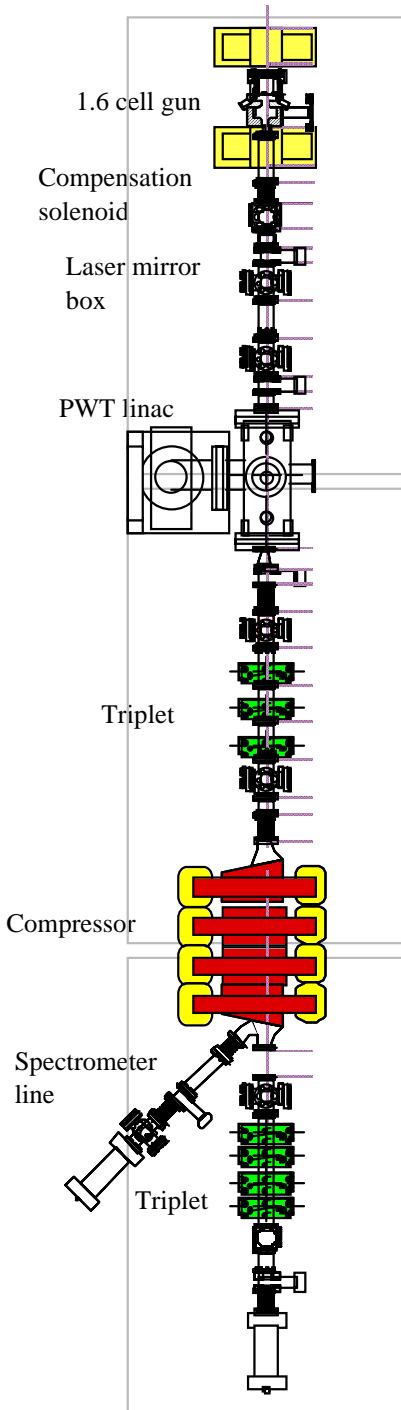


Figure 1. The Neptune photoinjector at UCLA.

($\omega_p = k_\beta c$). Thus the beam edges, which define angles in phase space, line up, regardless of slice, twice per oscillation, at the beam minimum and maximum. At these points, the projected emittance is also a minimum. The process of emittance compensation is essentially the arresting of these oscillations after an integer number of beam plasma periods. The plasma oscillations are adiabatically terminated, of course, by acceleration, which diminishes the strength of the space-charge.

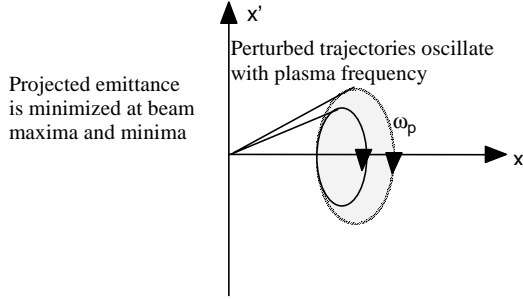


Figure 2. Emittance oscillations caused by slices about rotating in phase space about different equilibria.

The recently developed analytical theory of emittance compensation is based on Eq. 6, and examines a new type of equilibrium laminar flow (analogous to Brillouin flow) the invariant envelope [12]

$$\sigma_{\text{inv}} = \frac{2}{\gamma'} \sqrt{\frac{I}{3I_0\gamma}} \quad (8)$$

The invariant envelope has the property that the phase space angle $\sigma'_{\text{inv}}/\sigma_{\text{inv}} = \gamma'/2\gamma$ is independent of current. This guarantees that once all slices are aligned in phase space, they remain so. Slices not aligned to the invariant envelope oscillate in a Liouvillian space about the invariant envelope, giving rise to emittance oscillations. It should also be noted that the beam becomes smaller as it accelerates, driving the residual emittance down as $\gamma^{-1/2}$.

The model for the compensation of time-dependent space-charge forces is well understood analytically, through simulation, and experiment. New theoretical work concerning the role of nonlinear forces in optimized beam transport, is now underway.

3.3 Scaling of Designs

One recent advance in the understanding of photoinjector beam physics is the development of charge (Q) and wavelength (λ) scaling laws [14]. Charge scaling allows change of design charge while keeping dynamics of compensation identical, thus permitting a high Q , low brightness design (e.g. TTF) to a low Q , high brightness design (e.g. TTF-FEL). Wavelength scaling allows the taking of a design from one rf wavelength, and move it to a different value of λ . This permits expertise to be shared among different laboratories, and the performance of seemingly disparate devices to be compared. It also is a tool which can, as we will see below, point to promising new directions in source development.

In charge scaling, we do not change external forces (or wave-numbers), and must therefore preserve plasma wave-number. This in turn implies that we preserve bunch density and aspect ratio, or $\sigma_t \propto Q^{1/3}$. Deviations from strict Q -scaling arise from space charge at cathode, and rf effects, as the beam size changes relative to rf wavelength. Following this scaling, it can be shown that the emittance arises from two components: space-charge, which contributes $\epsilon_x^{\text{sc}} \propto \sigma_x^2 \propto Q^{2/3}$, and rf/chromatic focusing effects, which contribute $\epsilon_x^{\text{rf}} \approx \sigma_z^2 \sigma_x^2 \propto Q^{4/3}$. PARMELA simulations of a family of Q -scaled cases in an S-band emittance compensated injector gives the results shown in Fig. 3.

The fit for the data shown is

$$\epsilon_x \equiv \sqrt{\frac{4}{5} Q^{4/3} + \frac{1}{2} Q^{8/3}} \quad (9)$$

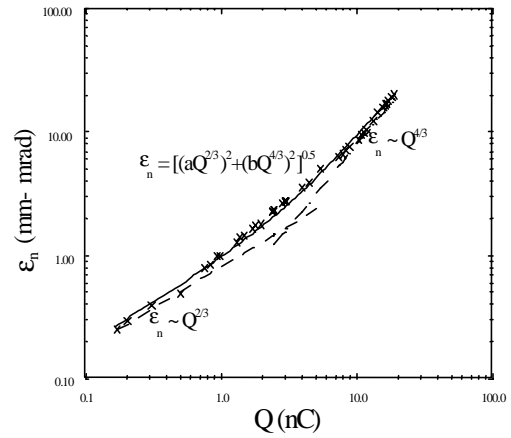


Figure 3. Emittance for family of Q -scaled cases in an S-band emittance compensated injector.

For wavelength scaling, we must preserve longitudinal dynamics, which requires $\alpha = \text{constant}$, or $E_0 \propto \lambda^{-1}$. To additionally preserve the energy spread and beam aspect ratio, we have that all beam dimensions scale as $\sigma_i \propto \lambda$. Further, making the betatron frequency scale properly requires that the solenoid field $B_0 \propto \lambda^{-1}$, and the scaling of the beam-plasma frequency requires $Q \propto \lambda$.

There are no inherent deviations from λ -scaling laws, and use of these laws can be shown to yield an emittance scaling of $\epsilon_x \propto \lambda$. Note also, that brightness scales as $B \propto \lambda^{-2}$; the advantage of short λ operation is apparent.

Nevertheless, several aspects of scaling to short λ merit discussion. Technologically, the laser pulse length and jitter are as well as emittance measurements are more difficult at short λ . The scaling of external forces requires large rf fields, which may be “natural” - high-gradient implies short λ because of breakdown limits, power considerations, etc. The scaling of the focusing fields is less natural, however, as the current density in the solenoid scales as $J_{\text{sol}} \propto \lambda^{-2}$. In addition, many applications require a certain charge per bunch. With large charge, short wavelength implies rf dominated operation. The optimum emittance and brightness occur

at a certain wavelength in the transition between the space-charge and rf-dominated regimes — for $Q=1$ nC, the optimum deduced from Eq. 9 is approximately 9 GHz.

4 TECHNOLOGY

Many of the performance limitations in photoinjectors are technological, not fundamentally physical. We now review the status of rf photoinjector technologies.

4.1 RF cavities

Rf cavities for photocathode gun use have gone through considerable development in the last decade. The most successful designs have been the low- α , integrated photoinjectors typified by the LANL devices, and the high- α short (1.5-6 cell) guns pioneered at BNL.

The high- α S-band gun has been improved recently by making the photocathode cell of length 0.625 times a π -mode standing wave cell. This improves the ratio of peak on-axis to wall fields, and provides stronger rf focusing near the cathode, enhancing the emittance compensation process. The coupling to the waveguide is performed only in the full cell, using symmetrized slots or a coaxial coupler, with on-axis coupling to the 0.5-cell.

The integrated photoinjector, in which a large number of cells are coupled together, cannot be easily coupled on axis in the π -mode while maintaining good mode separation. The solution employed at LANL entails coupling through on-axis vestigial cells in a $\pi/2$ -mode configuration. A new S-band design being pursued by a UCLA/DULY Research collaboration uses a plane wave transformer (PWT) structure. This structure has excellent coupling through a coaxial region outside of the accelerating mode-supporting disks. The emittance compensation optics in this device were the first to be derived from analytical theory [12]. It is interesting to note, however, that the optics in the PWT could have been deduced by scaling of the L-band optics of the AFEL injector at LANL — they are nearly identical when scaled. Scaling of the PWT design to X-band is in fact discussed below.

4.2 Lasers

Several years ago, the necessary drive laser pulses (picoseconds, total energy from tens of μ J to tens of mJ) were very difficult to achieve [14]. The amplification process often used flash-lamp pumping and chirped-pulse amplification, both of which tend to introduce unwanted fluctuations in pulse energy. This problem has been mitigated by use of diode-pumping technology. Advanced development in photocathode drive lasers now concentrates on production of long pulse trains [15], and on obtaining an illumination which is relatively uniform in time and transverse position, to make the space-charge forces as linear as possible. This goal may now be in reach through use high-bandwidth, short pulse lasers (*e.g.* Ti:Sapphire) combined with Fourier-plane filtering, as well as soft aperturing and relay imaging of the pulse.

4.3 Photocathodes

The search for a robust, high quantum efficiency (QE) cathode is now localized on two types of materials. Metals such as magnesium have been found to be prompt, with fsec response, but with QE no better than 10^{-3} (with uv illumination) and significant dark current. In addition, metal cathodes are surprisingly sensitive to vacuum conditions, and typically must be “laser cleaned” to produce anything approaching uniform emission.

A more promising candidate for high-brightness cathode development is Cs₂Te. This material is relatively immune to vacuum problems, can be revived after contamination, has QE as large as 15%, and a low inherent emittance. On the other hand, it still requires uv illumination to photo-emit, and is undoubtedly slower in emission delay than a metal photocathode.

Linear collider electron sources demand polarization. The development of a polarized photocathode in an rf gun, which entails addressing vacuum, field, and charge limitation problems, is only now beginning. Testing of GaAs cathodes in a high gradient rf gun has been reported at the CLIC Test Facility [16].

5 PRESENT PERFORMANCE

The state-of-the-art in beam parameters obtained from rf photoinjectors has advanced rapidly in the last few years.

- The charge measured from these devices has been as high as 100 nC [16,17]. Pulse trains with as much as mC have been reported.
- The pulse length, which is typically space-charge limited, has been measured at the level of a picosecond, for relatively low charge. For higher charge, the highest current reported is a few kA [16]. Picosecond pulses can be measured by streak cameras (which also provide imaging information) or rf sweeping techniques. At this pulse length, and below, it is now popular to use coherent transition radiation interferometry, which can resolve times as small as 0.2 psec.
- The normalized rms emittance has been measured in a variety of laboratories [18] to be at the level of 2 mm-mrad/nC. This is expected to be reduced by a factor of two with the advent of shaped laser pulses. The measurement of the emittance in space-charge dominated beams has presented a challenge in its own right, with the standard quadrupole scan method being prone to space-charge induced problems in interpretation. Nevertheless, at BNL these problems have been overcome, and a time-resolved emittance measurement, which verified the slice-model of emittance compensation reported [19]. Alternatively, a slit-based measurement system can be employed which mitigates space charge and allows single shot reconstruction of the beam’s phase space.

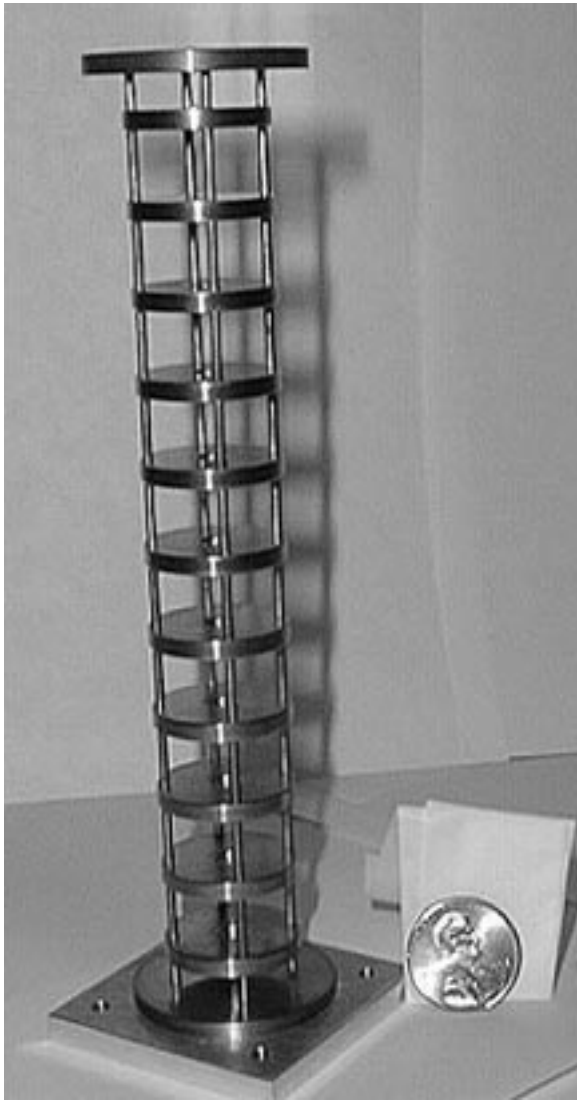


Figure 4. Interior of 11.4 GHz PWT cold test structure.

6 FUTURE DIRECTIONS

The choice between integrated and split photoinjectors is not simple, as there are advantages and unattractive features to both. The split photoinjector is flexible; one can choose booster linac gradient/phase, and gun-linac drift length for compensation can be optimized. One can naturally include a compressor. One actually must choose a high gradient in the gun, or the drift section will produce pulse lengthening and larger residual transverse emittance — the TTF gun is run at relatively α . As the defocusing kick at the gun exit is proportional to the beam size, the compensation solenoid must be stronger, and is difficult to build at short λ . Also because of the exit kick, the beam size oscillation is larger, and this produces larger residual emittances.

For an integrated injector, the gradient in the structure is lower, and the scaling to short λ is easier. At lower gradient however, the space-charge pulse lengthening near the cathode is larger than that in a high-gradient gun, but because of continuously applied longitudinal focusing in the structure, the bunch does not appreciably lengthen

after the initial cell. The needed solenoid field lower is also lower, again allowing easier scaling to short λ . As the beam exits the structure small (near the invariant envelope) the rf kick at the structure exit is not large, and the rf-derived emittance can be greatly mitigated.

It can thus be seen that the high gradient gun generally produces shorter pulse lengths, but the integrated injector gives better emittance performance at a given λ . But if one chooses a short λ , then the achievable pulse length becomes smaller. Because of this, we have proposed, and are now seriously developing a scaled X-band version of the PWT injector at UCLA, in collaboration with DULY Research and LLNL. Simulations of an 11.4 GHz injector indicate [5] that this device can produce 120 μm rms bunch lengths at 1 nC, with $\epsilon_n = 0.8$ mm-mrad, for a brightness, $\epsilon_n = 3 \times 10^{15}$ cm^{-2} , which is a factor of 30 times greater than the present state of the art. In this development we are concentrating on the issues of structure cooling and solenoid design, which both become quite challenging in X-band. A cold-test model of an 11.4 GHz structure's interior is shown in Fig. 4. Development of the injector will probably take place at 8.6 GHz, however, due to availability of rf power, and solenoid design issues. It should also be noted that this is near the optimum value of λ predicted to minimize the emittance at 1 nC.

7 REFERENCES

- [1] M.Hogan, et.al, *Phys. Rev. Lett.* **80**, 289 (1998)
- [2] R. W. Schoenlein, et al., *Science* **274**, 236 (1996).
- [3] W. Gai, et al., *Phys. Rev. Lett.* **61**, 2765 (1988).
- [4] H. Tang, et al, 1997 Part. Accel. Conf. 2849 (1998).
- [5] J. Rosenzweig, et al., *Proc. 1997 Part. Accel. Conf.* 1965 (1998).
- [6] J. Rosenzweig, et al., *NIM A* **410**, 437 (1998).
- [7] J.B. Rosenzweig, N. Barov and E. Colby, *IEEE Trans. Plasma Sci.* **24**, 409 (1996).
- [8] K.J. Kim, *NIM A* **275**, 201 (1989).
- [9] B.E. Carlsten and T.O. Raubenheimer, *Phys. Rev. E* **51**, 1453 (1995).
- [10] J. Rosenzweig and L. Serafini, *Phys. Rev. E* **49**, 1499 (1994).
- [11] S. Reiche, et al., *Phys. Rev. E* **56**, 3572 (1997).
- [12] Luca Serafini and James Rosenzweig, *Phys. Rev. E* **55**, 7565 (1997).
- [13] J. Rosenzweig, and E. Colby, *Proc. 1995 Advanced Accelerator Concepts Workshop 337* (AIP, 1996).
- [14] See *Proc. Lasers for RF guns*, Brookhaven National Laboratory Report, 1994.
- [15] TESLA Test Facility Design Report, D.A. Edwards, Ed. TESLA Rep. 95-01 (Hamburg, 1995).
- [16] E. Chevallay, et al., these proceedings.
- [17] M.E. Conde, et al, *Phys. Rev. ST-Accel. Beams* **1**, 041302 (1998)
- [18] D.T. Palmer, et al., *Proc. 1997 Part. Accel. Conf.* 2687 (1998).
- [19] X. Qiu, et al, *Phys. Rev. Lett.* **78**, 3723 (1996).